Pharm Res (2011) 28:2945–2953
DOI 10.1007/s11095-011-0463-0

RESEARCH PAPER

Improvement of Cerebral Metabolism Mediated by Ro5-4864 is Associated with Relief of Intracranial Pressure and Mitochondrial Protective Effect in Experimental Brain Injury

Jean F. Soustiel • Eugene Vlodavsky • Felix Milman • Moshe Gavish • Menashe Zaaroor

Received: 18 February 2011 / Accepted: 26 April 2011 / Published online: 17 May 2011

ABSTRACT

Purpose To investigate the possible impact of reduction of mitochondrial membrane permeabilization by modulation of the 18 kDa translocator protein mediated by Ro5-4864 over post-traumatic cerebral edema and metabolic crisis.

Methods Cerebral microdialysis and intracranial pressure (ICP) monitoring were performed in Sprague–Dawley rats treated by intraperitoneal injection of either dimethylsulfoxide (vehicle) or Ro5-4864 following cortical contusion and further correlated with quantitative assessment of mitochondrial damage, water content in the injured tissue, modified neurological severity score, and lesion size.

Results Ro5-4864 resulted in a profound decrease in ICP that correlated with improved cerebral metabolism characterized by significantly higher glucose and pyruvate and lower lactate concentrations in the pericontusional area in comparison with vehicle-treated animals. Reduced ICP correlated with reduced water content in the injured tissue; improved metabolism was associated with reduced mitochondrial damage evidenced by electron microscopy. Both effects were associated with a profound and significant reduction in glycerol release and lesion size, and correlated with improved neurological recovery.

Conclusions The present study shows that Ro5-4864 has a favorable effect on the fate of injured brain, presumably mediated by improvement of metabolism. It further suggests that improvement of metabolism may contribute to ICP relief.

KEY WORDS 18 kDa translocator protein · intracranial pressure · microdialysis · mitochondria · traumatic brain injury

INTRODUCTION

Elevation of intracranial pressure (ICP) due to brain edema and failure of oxidative metabolism is commonly observed following severe traumatic brain injury (TBI) (1,2). Decreased oxidative metabolism has been traditionally linked to compromised cerebral perfusion due to elevated ICP and reduced oxygen delivery (1,3). Recent studies indicate, however, that failure of cerebral metabolism is not necessarily mediated by ischemia but more likely represents the consequence of mitochondrial damage and disruption of the electron transport chain (4–6). Energy crisis, in turn, results in failure of ATP-dependent ionic pumps, further contributing to cellular edema and ICP elevation. Hypothetically, metabolic crisis may therefore share a common pathophysiology with intracranial hypertension rather than being a consequence of it. Such hypothesis is supported by the reported fact that oxidative metabolism does not

Eugene Vlodavsky made an equal contribution to this work.

J. F. Soustiel · F. Milman · M. Zaaroor
Acute Brain Injury Research Laboratory, Faculty of Medicine
Technion — Israel Institute of Technology
Haifa, Israel

E. Vlodavsky
Institute of Pathology, Rambam Medical Center, Faculty of Medicine
Technion — Israel Institute of Technology
Haifa, Israel

M. Gavish
Department of Molecular Pharmacology, Faculty of Medicine
Technion — Israel Institute of Technology
Haifa, Israel

J. F. Soustiel (✉)
Department of Neurosurgery, Rambam Medical Center
P.O.B. 9602, Haifa 31096 Israel
e-mail: j_soustiel@rambam.health.gov.il

improve as a consequence of optimization of cerebral perfusion pressure, often as it deteriorates with ICP elevation (4,5,7,8).

Under physiological conditions, ATP is produced by the ATP synthase complex using a proton gradient created by the electron transport chain across the outer mitochondrial membrane, resulting in a potential known as transmembrane mitochondrial potential ($\Delta\psi_M$). Across the mitochondrial membrane is a complex of proteins creating a physiological and selective crossing channel between the mitochondrial matrix and the cytosol, known as the mitochondrial permeability transition pore (mPTP). The mPTP is normally characterized by a low conductance profile maintaining a normal $\Delta\psi_M$. Accumulating evidence shows that mitochondrial damage represents a crucial step toward delayed neuronal death following TBI, both as a target for multiple pathophysiological subcellular events, such as free radicals and calcium load, and as the source of activation of the so-called intrinsic apoptotic pathway (9–11). Despite the different nature and the origin of these mechanisms, most are characterized by permeabilization of the mitochondrial membrane (MMP) with subsequent dissipation of $\Delta\psi_M$ and disruption of ATP production and may, therefore, represent a logical target for new therapeutic strategies (9,11–14). The 18 kDa translocator protein (TSPO), also known as peripheral-type benzodiazepine receptor, is a binding protein complex (15) located at the outer mitochondrial membrane and associated with two core components of the mPTP: the 32-kDa voltage-dependent anion channel and the 30-kDa adenine nucleotide translocator (16). For this reason, it has been suggested that TSPO may be involved with the control of the mPTP and the mitochondrial pathway of apoptosis (17). In a recent study (18), we showed that the TSPO ligand 7-chloro-5-(4-chlorophenyl)-1,3-dihydro-1-methyl-2H-1,4-benzodiazepine-2-one (Ro5-4864) significantly enhanced neuron survival and reduced axonal damage in a rat model of focal TBI and loss of $\Delta\psi_M$. Accordingly, we hypothesized that inhibition of MMP by Ro5-4864 may improve cerebral metabolism and contribute to ICP control through reactivation of ionic pumps.

MATERIAL AND METHODS

In Vivo Study

Surgical Procedures

Following anesthesia with equithesin (4 ml/kg of body weight), a cortical traumatic injury was created in male Sprague–Dawley rats (300–350 g) using a model used in several earlier studies (19–21) and modified for amplification of focal damage. Briefly, a hollow screw was connected to a 7 mm diameter burr hole drilled out in the left parietal bone and then to vacuum pump after resection of the exposed dura. A negative pressure of 160 mm Hg was then applied for 12 s, causing the cortical surface to bulge into the lumen of the screw. The pressure was monitored and the time of exposure digitally controlled. Following the injury, the wound was sutured and the animals allowed to recover. The study was approved by the institutional Animal Care and Ethics Committee and adhered to the "Principles of Laboratory Animal Care."

Microdialysis and Intracranial Pressure Monitoring

Two groups of animals were included in this study. Group 1($N=8$)—vehicle: 30 min after injury, the animals received an intraperitoneal injection of dimethylsulfoxide 1% in saline (vehicle) repeated at 6 h post injury; Group 2($N=8$)—Ro5-4864: using the same protocol as for group 1, the animals were treated with 5 mg/kg of Ro5-4864 dissolved in vehicle. Timing of drug administration for the first dose was set to the shortest possible time post injury that could be performed in clinical conditions (pre-hospital model) and then at 6 h for the second dose in order to increase the therapeutic effect in accordance with a previously reported similar protocol (22). Dosage of Ro5-4864 was defined as the highest possible dosage compatible with absence of toxicity, since dosage higher than 5 mg/kg has been found to cause epileptic seizures (23,24).

Based on previous clinical experience (25) and the reported time course for ICP elevation, the rationale for limiting the time range of monitoring to the first 10 to 12 h, as previously reported in several similar studies, seemed to be inappropriate for the purpose of the present study. Accordingly, both ICP and cerebral metabolism recordings were initiated at 20 h post-injury and maintained for 6 h. For this purpose, the animals were re-anesthetized, the wound opened, and the screw reconnected to the skull. A Codman ICP microsensor (Codman, Johnson and Johnson, Ascot, UK) was introduced through the screw and allowed to protrude 2 mm within the injured brain. The microsensor was thereafter connected to a Codman ICP monitoring system for continuous ICP recording. In addition, a microdialysis catheter (CMA 12, CMA Microdialysis, Sweden) was introduced through a guide cannula secured in a dedicated and distinct burr hole placed 2 mm anteriorly to the craniectomy. Perfusion was then initiated at 1 µl/min with CNS perfusion fluid (CMA Microdialysis, Sweden) and microdialysis samples collected on ice every hour. Concentrations of glucose, lactate, pyruvate and glycerol were measured using high performance liquid chromatography (CMA 600, CMA Microdialysis, Sweden) and averaged hourly for statistical analysis. Similarly, ICP

levels were recorded every 5 min and averaged hourly for the same period of 6 h.

Neurological Severity Score

Functional performance status was assessed blindly from day 1 to day 6 post injury, according the neurological severity score (NSS) described by Shohami *et al.* (26) and simplified as described in Table I. In order to rule out a possible behavioral bias in the evaluation, animals were trained on a daily basis to all the described tasks prior surgery and all reached a maximal score.

Ex Vivo Study

Lesion Area Analysis

Using the same study design described above, two groups of eight animals each were submitted to cortical injury and treated either with vehicle or Ro5-4864 with two intraperitoneal injections at 30 min and 6 h post injury according the *in-vivo* protocol. At 6 weeks, the animals were re-anesthetized and transcardially perfused with heparinized saline, 10% sucrose in a buffered saline and 4% buffered formaldehyde. This delayed timing was chosen as both the necrotic area and surrounding edema cleared, leaving a cavity convenient for unbiased evaluation of lesion size. Brains were then removed from the skull and post fixed by immersion into 4% buffered formaldehyde for 48 h. Fixed specimens were sectioned through the area of the produced lesion and embedded in paraffin. Coronal sections of 5 µm thickness were cut throughout the lesion every 0.20 mm. The images of the stained specimens were captured by a digital photo camera and analyzed by image processing software (NIH Image J, National Institutes of Health, USA). The cross-sectional area of the injured and non-injured hemispheres was determined by tracing the remaining cortical area in a blinded fashion, according to a previously described technique (27). At each section, the area of the traumatic cavity was estimated by subtracting the area of the injured hemisphere from that of the contralateral hemisphere. The three consecutive largest measured areas were selected for analysis and averaged.

Table I Modified Neurological Severity Score

Tasks	mNSS score
Inability to walk straight when placed on the floor	1
Inability to resist forced changes in position	1
Absence of pinna reflex	1
Absence of startle reflex	1
Loss of seeking behavior	1
Prostration	1
Failure in beam walking task:	
8.5 cm wide	1
5 cm wide	1
2.5 cm wide	1
Failure in 1.5-cm-wide beam balancing task	1
Maximum points	10

Mitochondrial Morphometric Assessment

Tissue samples ranging in weight from 100 to 150 mg were harvested from the parietal region in three different groups of animals: untreated and uninjured (sham, $N=4$), injured and vehicle-treated ($N=4$), injured and Ro5-4864-treated ($N=4$). In the last two groups, tissue samples were prepared 24 h post injury. Tissue samples were washed in phosphate buffer solution for 5 min at 4°C and then handled using a specially designed mitochondria isolation kit (Mito-Iso1, Sigma-Aldrich, Saint Louis, MO) according to the manufacturer's instructions. Briefly, the collected tissue was homogenized on ice with 10 volumes of ice-cold extraction buffer (10 mM HEPES, pH 7.5, containing 200 mM mannitol, 2 mg/ml bovine serum albumin, 70 mM sucrose and 1 mM EGTA) and centrifuged at 1,000 × *g* for 10 min at 4°C. The pellets were discarded and the supernatant re-centrifuged at 3,500 × *g* for 10 min at 4°C. Pellets obtained from this centrifugation were re-suspended with 10 volumes of a second ice-cold extraction buffer (20 mM MOPS, pH 7.5, containing 110 mM KCl and 1 mM EGTA) and treated by sequential centrifugation as above.

The obtained pellets were layered with 3.5% glutaraldehyde in 0.2 mol/L sodium cacodylate buffer and left overnight at 4°C. The samples were then postfixed in 1% osmium tetroxide and embedded in epoxy resin. Quantitative morphometric assessment was then performed for each group with transmission electron microscopy (TEM) using micrographs acquired at low magnification (×6000) obtained from eight randomly chosen areas in the grid. Mitochondria were analyzed and categorized according their ultrastructural appearance into two categories, condensed or damaged, according a previously described protocol (28). Condensed mitochondria were defined by normal appearance of matrix cristae and a continuous outer membrane, whereas damaged mitochondria were classified primarily by fragmented cristae with evidence of either a swollen distorted matrix compartment or disrupted outer membrane.

Water Content

In order to quantify the brain water content for the two different protocols (vehicle and Ro5-4864), tissue samples

from both hemispheres (injured and non-injured) were harvested in a symmetric fashion and then weighted before and after drying at 75°C for 48 h. Water content was then calculated according the following formula: wet − dry/dry × 100.

Statistical Analysis

The results of all repeated measures in the different groups were compared with a repeated-measures model of ANOVA (rm-ANOVA). Results of mitochondrial ultrastructural assessment were assessed with a one-way model of ANOVA. Whenever appropriate, post-hoc analysis of differences noted between two groups of animals were tested using the Tukey-Kramer multiple comparison post-hoc test. Differences in lesion size and water content were assessed by *t*-test. A P value of less than 0.05 was considered significant.

RESULTS

In Vivo Study

ICP

At 20 h after the injury, ICP was noticeably high in the vehicle group, close to the 20 mm Hg threshold usually admitted for definition of uncontrolled ICP elevation (Fig. 1). In the treated group, however, ICP was significantly and profoundly reduced, less than half the ICP level recorded in vehicle-treated animals (8.4±1.1 *vs* 19.9± 2 mm Hg, repeated measures ANOVA, combined effect of time and group, $p=0.0313$).

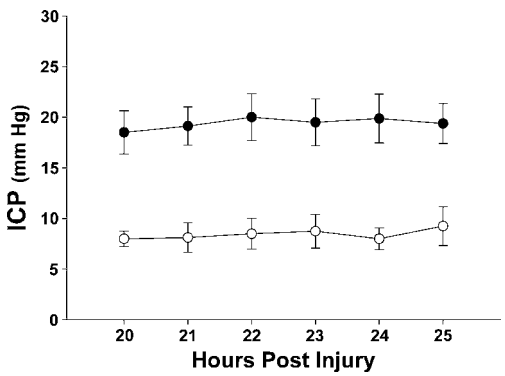

Fig. 1 Effect of Ro5-4864 on ICP. Ro5-4864-treated animals ($N=8$, *white dots*) showed markedly lower ICP values at 20 h post injury in comparison with vehicle-treated animals ($N=8$, *black dots*). For each hour, average ICP values are presented along with the standard error of the mean.

Microdialysis

Glucose levels were significantly and profoundly lower in the vehicle group in comparison with the Ro5-4864 group (rm-ANOVA, main effect of group $p=0.0002$, Fig. 2). Indices of oxidative metabolism showed a marked reduction of the injury-mediated metabolic crisis in Ro5-4864-treated rats in comparison with the control group, indicated by lower levels of lactate and higher levels of pyruvate (rm-ANOVA, main effect of group, $p=0.0179$ and $p=0.0216$, respectively). As a consequence, the lactate/pyruvate ratio (LPR) was noticeably lower in the Ro5-4864 group with values constantly below the LPR-40 threshold considered as a cut-off diagnostic value of metabolic failure, in contrast with the vehicle group characterized by increased LPR values mostly around 100(rm-ANOVA, main effect of group $p=0.0062$). Finally, glycerol levels were markedly lower in the treated group in comparison with non-treated animals that were roughly twice the value found in Ro5-4864-treated animals (rm-ANOVA, main effect of group $p=0.0002$, Fig. 2).

Neurological Recovery

Following the injury, there was a progressive recovery of motor and behavioral functions expressed by decrease in the modified neurological severity scores in both groups. Ro5-4864-treated animals, however, showed a significantly faster and better neurological recovery in comparison with vehicle-treated rats, which had a significantly lower performance status at day 6 (Fig. 3).

Ex Vivo Study

Lesion Area

Reduced glycerol levels in the treated group were associated with a substantial decrease of secondary brain injury expressed by the size of the final traumatic cavity that was about half the size of the lesion as measured in vehicle-treated animals (Fig. 4, *t*-test $p<0.001$).

Mitochondrial Morphometric Assessment

Injury-related mitochondrial damage was characterized by a marked and significant reduction in mitochondrial density in vehicle-treated animals (Fig. 5b) with an increased proportion of swollen, damaged and disrupted mitochondria (Fig. 5e). Although changes similar in nature could be noticed in samples collected in Ro5-4864-treated animals, the severity of mitochondrial damage was significantly reduced (Fig. 5c, f) and the number of damaged mitochondria significantly lower in comparison

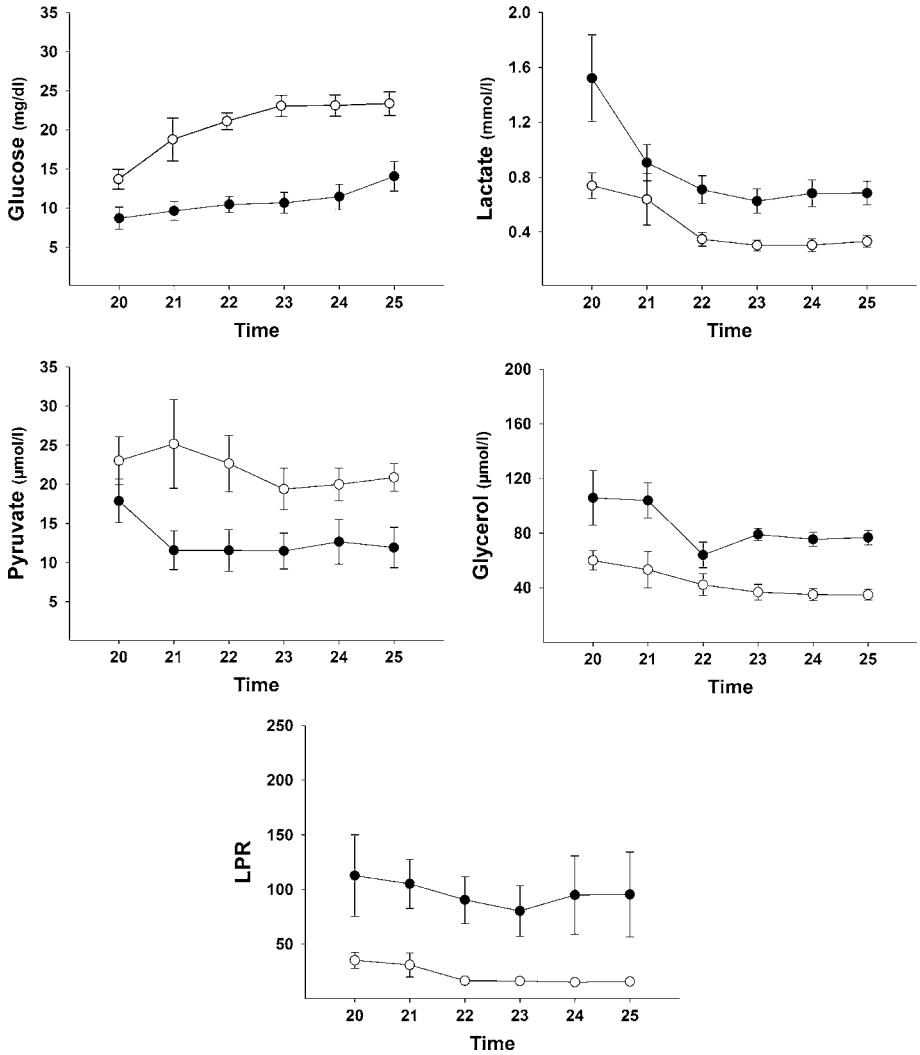

Fig. 2 Effect of Ro5-4864 on cerebral metabolism. Microdialysis study was initiated at 20 h post injury and maintained for 6 h. Ro5-4864-treated animals ($N=8$, *white dots*) were characterized by higher glucose and pyruvate levels, lower lactate and lactate/pyruvate ratios levels than those found in non-treated animals ($N=8$, *black dots*). Improved metabolic indices correlated with glycerol levels markedly lower in the treated group in comparison with non-treated animals that were roughly twice the value found in Ro5-4864- treated animals. Hourly-averaged values are presented with the standard error of the mean for each investigated metabolite.

with vehicle-treated animals (Fig. 6, one-way ANOVA, $p<0.0001$).

Water Content

In animals treated by Ro5-4864, reduced mitochondrial damage and ICP correlated with significantly lower water content in the injured hemisphere of treated animals in comparison with the control group (Fig. 7, *t*-test $p<0.001$).

DISCUSSION

For decades, the cornerstone of TBI management has been represented by relief of brain edema and ICP control, assuming that these measures would eventually result in optimization of oxygen delivery and cerebral metabolism. Based on the Monro-Kellie theory and basic pressure-volume concepts, most current therapeutic measures are mechanistic in nature and rely on either reduction of various intracranial compartment volumes or expansion of the intracranial space by means of decompressive craniectomy. None of these treatment modalities, however, directly addresses the underlying pathophysiology of brain edema and at most would only target its physicochemical aspects such as reduction of brain water content by means of hypertonic fluids. Even if mechanically successful, the concept of ICP control for improvement of cerebral blood flow and metabolism has been recently challenged by a series of recent clinical studies showing that the cerebral metabolic rate of oxygen could not be improved as a result of ICP decrease (4,7,8,29). In these studies, neither optimization of cerebral perfusion pressure, hyperventilation, infusion of hypertonic solutions or decompressive craniectomy showed any significant improvement in oxygen consumption by the injured brain, even though cerebral blood flow could be effectively maintained or elevated by some of these measures. Furthermore, in a recent microdialysis study performed in TBI patients, Belli *et al.* showed that metabolic crisis preceded ICP rises that could not,

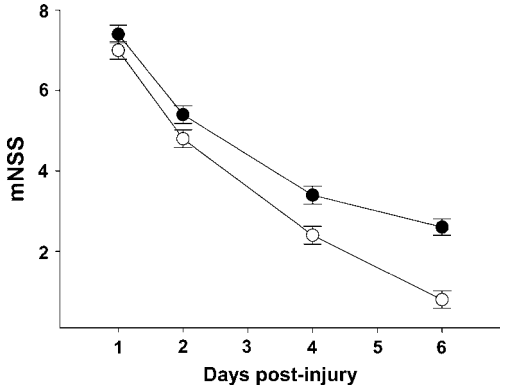

Fig. 3 Effect of Ro5-4864 on modified neurological severity score (mNSS). Although neurological recovery expressed by progressive mNSS decrease could be observed in both groups after the injury, Ro5-4864-treated animals ($N = 8$, *white dots*) showed a significantly faster and better neurological recovery in comparison with vehicle-treated rats ($N = 8$, *black dots*), which have a significantly lower performance status at day 6. Averaged mNSS are presented along with the standard error of the mean for each point.

therefore, represent the cause of the observed metabolic failure (30).

The results of the present study do not only confirm the previously reported mitochondrial protective effect of Ro5-4864 but also show that improvement of cerebral metabolism correlated with a robust effect on ICP. In our previous study, we showed that Ro5-4864 significantly reduced the loss of mitochondrial transmembrane potential induced by Bax, a major pro-apoptotic protein of the Bcl-2 family, and the subsequent activation of the mitochondrial pathway of apoptosis attributed to MMP-induced release of apoptotic factors such as cytochrome c (18). In the present study, we could directly evidence this mitochondrial protective effect by showing a significant reduction in the extent and severity of mitochondrial ultrastructure alterations. This protective effect of Ro5-4864 correlated

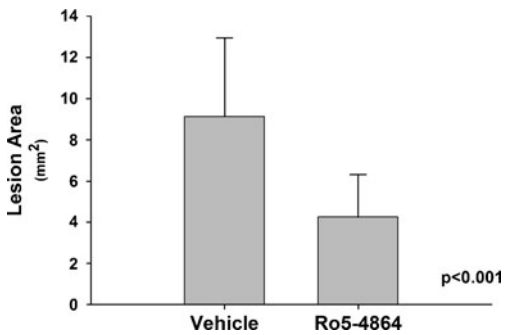

Fig. 4 Effect of Ro5-4864 on lesion size. Reduced glycerol levels in the treated group were associated with a substantial decrease of secondary brain injury expressed by the size of the final traumatic cavity that was about half the size of the lesion as measured in vehicle-treated animals. Averaged lesion sizes are presented along with standard deviation for each group.

with a profound decrease in the LPR ratio, usually considered as a surrogate of oxidative metabolism level. Interestingly, decrease in LPR proved to be the consequence of both lactate decrease and higher pyruvate levels. LPR elevations have been initially reported in correlation with brain ischemia (31), although in a later review, the same group of authors described two different types of LPR elevation reflecting two different pathophysiological situations (32). The type 1 or "classical ischemic metabolic state," characterized mostly by a marked lactate elevation, reflects a redox state where the lactate dehydrogenase reaction is profoundly shifted toward lactate production as a consequence of severely compromised oxygen delivery, as is the case in brain ischemia. The type 2 of increased LPR, in contrast, appears to be more frequent in TBI patients and is presumed to reflect a state of impairment of the aerobic glycolysis. This subtype of LPR elevation is characterized by a marked decrease in pyruvate rather than lactate elevation as in type 1 and has been reported in presence of normal brain tissue oxygen tension (33). In the present study, LPR decrease induced by Ro5-4864 could be equally attributed to both lactate decrease and pyruvate elevation, probably reflecting the protective effect of the drug at the mitochondrial level as well as the improvement of cerebral perfusion in the pericontusional area as a consequence of ICP decrease. This latter assumption is supported by the significant increase in extracellular levels of glucose, which is widely admitted as a marker of brain ischemia (34,35).

Importantly, both ICP decrease and metabolic optimization were associated with a profound decrease in glycerol interstitial levels. Intracellular accumulation of calcium, free radical production and energy crisis have proved to trigger phospholipase activation, resulting in degradation of the phospholipid membrane with subsequent glycerol release (36), which was therefore suggested as a marker for membrane damage in cerebral ischemia (37). Considering the role played by alteration of membrane integrity in the induction of post traumatic cellular swelling (38), the profound reduction in glycerol levels found in treated animals supports the hypothesis that ICP reduction mediated by Ro5-4864 represents the consequence of improved capability of cells to maintain their membrane integrity, presumably as a consequence of an improved energy state. This assumption is supported by the significant reduction in water content observed in Ro5-4864-treated animals. Eventually, reduced glycerol release in treated animals correlated with a significant reduction in the lesion size that supports previous observations of enhanced neuronal survival and reduced axonal damage induced by Ro5-4864 caused by traumatic (18) and chemical brain injury (39). This

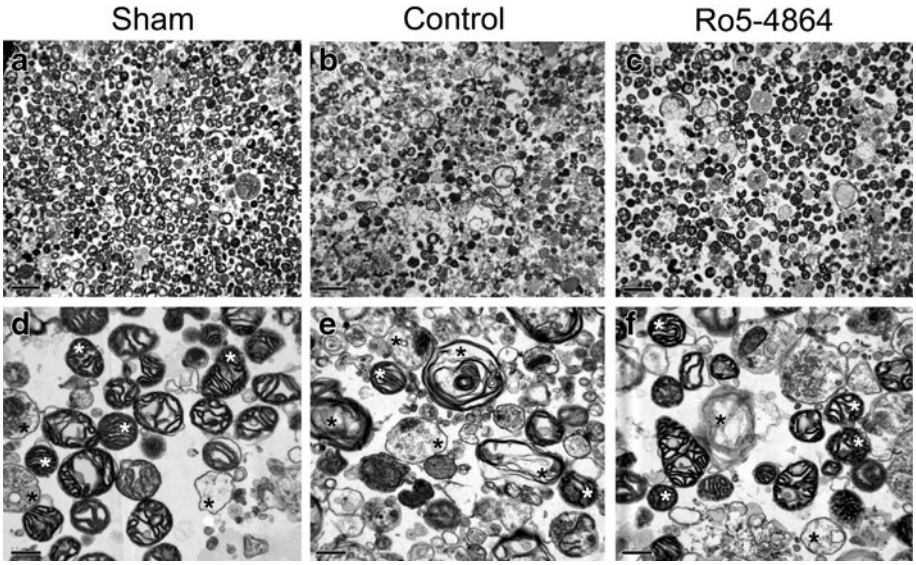

Fig. 5 Effect of Ro5-4864 on mitochondrial damage: electron microscopy. In comparison with sham animals (**a**), samples prepared from injured brain were characterized by a marked and significant reduction in mitochondrial density particularly evident at low magnification (**b**, upper left and lower right corners: ×6000). At higher magnification (×25000), mitochondrial damage was prominent in the injured group (**e**), with an increased proportion of swollen, damaged and disrupted mitochondria (*black asterisks*) with very few mitochondria retaining a normal appearance (*white asterisks*). Although changes similar in nature could be noticed in samples collected in Ro5-4864-treated animals, the severity of mitochondrial damage was significantly reduced (**c**, **f**). Symbols: *black asterisks*—damaged mitochondria characterized by fragmented cristae, swollen distorted matrix compartment or disrupted outer membrane; *white asterisks*: condensed mitochondria with normal matrix. Scale: upper—2 μm; lower—0.5 μm.

reduction in the lesion size may, in turn, account for the better neurological recovery observed in animals of the Ro5-4864 group. It should be kept in mind, however, that cytogenic edema represents only one aspect of post traumatic edema, along with increased blood-brain barrier permeability, so that improvement of intracellular homeostasis should be as a potential additional therapeutic modality along with other measures intended to control blood-brain barrier permeability.

All together, the results of the present study suggest that targeting mitochondrial membrane permeabilization may represent an additional therapeutic avenue for ICP control by improving the energy status of injured cells and subsequently reinforce their capability to maintain internal homeostasis.

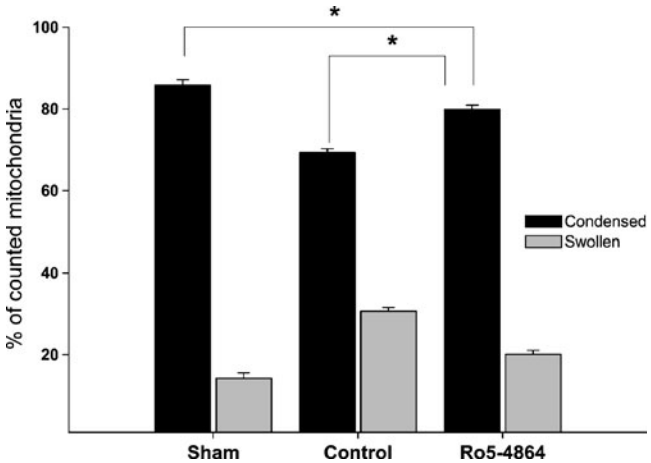

Fig. 6 Effect of Ro5-4864 on mitochondrial damage: summary. Analysis of 8 randomly chosen fields over the grid for each sample showed that the number of damaged mitochondria in Ro5-4864-treated animal was significantly lower in comparison with vehicle-treated animals. Averaged counts are presented along with the standard error of the mean for each group and type of mitochondria. *: one-way ANOVA, Tukey-Kramer pair-comparison test, $p < 0.05$.

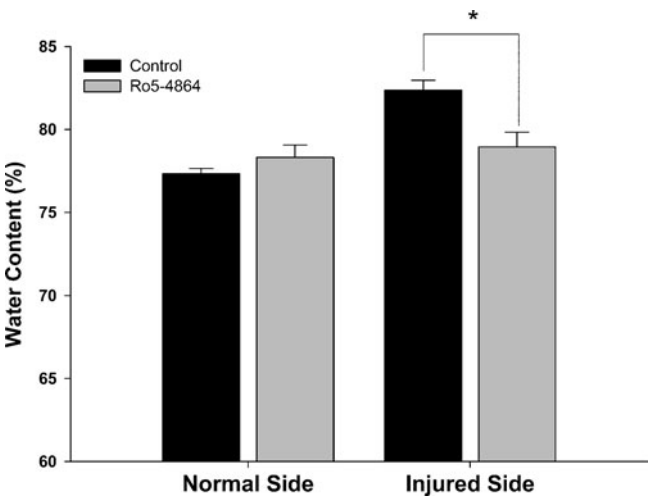

Fig. 7 Effect of Ro5-4864 on water content. Averaged water contents are presented along with the standard error of the mean for each group and side. *: *t*-test, $p < 0.0001$.

REFERENCES

1. Jaggi JL, Obrist WD, Gennarelli TA, Langfitt TW. Relationship of early cerebral blood flow and metabolism to outcome in acute head injury. J Neurosurg. 1990;72:176–82.
2. Obrist WD, Langfitt TW, Jaggi JL, Cruz J, Gennarelli TA. Relationship to intracranial hypertension. J Neurosurg. 1984;61:241–53.
3. Bouma GJ, Muizelaar JP, Bandoh K, Marmarou A. Blood pressure and intracranial pressure-volume dynamics in severe head injury: relationship with cerebral blood flow. J Neurosurg. 1992;77:15–9.
4. Chieregato A, Tanfani A, Compagnone C, Turrini C, Sarpieri F, Ravaldini M, *et al.* Global cerebral blood flow and CPP after severe head injury: a xenon-CT study. Intensive Care Med. 2007;33:856–62.
5. Soustiel JF, Sviri GE. Monitoring of cerebral metabolism: non-ischemic impairment of oxidative metabolism following severe traumatic brain injury. Neurol Res. 2007;29:654–60.
6. Vespa P, Bergsneider M, Hattori N, Wu HM, Huang SC, Martin NA, *et al.* Metabolic crisis without brain ischemia is common after traumatic brain injury: a combined microdialysis and positron emission tomography study. J Cereb Blood Flow Metab. 2005;25:763–74.
7. Soustiel JF, Mahamid E, Chistyakov A, Shik V, Benenson R, Zaaroor M. Comparison of moderate hyperventilation and mannitol for control of intracranial pressure control in patients with severe traumatic brain injury—a study of cerebral blood flow and metabolism. Acta Neurochir (Wien). 2006;148:845–51.
8. Soustiel JF, Sviri GE, Mahamid E, Shik V, Abeshaus S, Zaaroor M. Cerebral blood flow and metabolism following decompressive craniectomy for control of increased intracranial pressure. Neurosurgery. 2010;67:65–72. discussion 72.
9. Merenda A, Bullock R. Clinical treatments for mitochondrial dysfunctions after brain injury. Curr Opin Crit Care. 2006;12:90–6.
10. Robertson CL, Soane L, Siegel ZT, Fiskum G. The potential role of mitochondria in pediatric traumatic brain injury. Dev Neurosci. 2006;28:432–46.
11. Xiong Y, Gu Q, Peterson PL, Muizelaar JP, Lee CP. Mitochondrial dysfunction and calcium perturbation induced by traumatic brain injury. J Neurotrauma. 1997;14:23–34.
12. Galluzzi L, Blomgren K, Kroemer G. Mitochondrial membrane permeabilization in neuronal injury. Nat Rev Neurosci. 2009;10:481–94.
13. Mazzeo AT, Beat A, Singh A, Bullock MR. The role of mitochondrial transition pore, and its modulation, in traumatic brain injury and delayed neurodegeneration after TBI. Exp Neurol. 2009;218:363–70.
14. Soustiel JF, Larisch S. Mitochondrial damage: a target for new therapeutic horizons. Neurotherapeutics. 2010;7:13–21.
15. Braestrup C, Squires RF. Specific benzodiazepine receptors in rat brain characterized by high-affinity (3H)diazepam binding. Proc Natl Acad Sci USA. 1977;74:3805–9.
16. McEnery MW, Snowman AM, Trifiletti RR, Snyder SH. Isolation of the mitochondrial benzodiazepine receptor: association with the voltage-dependent anion channel and the adenine nucleotide carrier. Proc Natl Acad Sci USA. 1992;89:3170–4.
17. Decaudin D. Peripheral benzodiazepine receptor and its clinical targeting. Anticancer Drugs. 2004;15:737–45.
18. Soustiel JF, Zaaroor M, Vlodavsky E, Veenman L, Weizman A, Gavish M. Neuroprotective effect of Ro5-4864 following brain injury. Exp Neurol. 2008;214:201–8.
19. Palzur E, Vlodavsky E, Mulla H, Arieli R, Feinsod M, Soustiel JF. Hyperbaric oxygen therapy for reduction of secondary brain damage in head injury: an animal model of brain contusion. J Neurotrauma. 2004;21:41–8.
20. Soustiel JF, Palzur E, Vlodavsky E, Veenman L, Gavish M. The effect of oxygenation level on cerebral post-traumatic apoptotsis is modulated by the 18-kDa translocator protein (also known as peripheral-type benzodiazepine receptor) in a rat model of cortical contusion. Neuropathol Appl Neurobiol. 2008;34:412–23.
21. Vlodavsky E, Palzur E, Soustiel JF. Hyperbaric oxygen therapy reduces neuroinflammation and expression of matrix metalloproteinase-9 in the rat model of traumatic brain injury. Neuropathol Appl Neurobiol. 2006;32:40–50.
22. Lees GJ. Effects of anaesthetics, anticonvulsants and glutamate antagonists on kainic acid-induced local and distal neuronal loss. J Neurol Sci. 1992;108:221–8.
23. Nakamoto Y, Watabe S, Shiotani T, Yoshii M. Peripheral-type benzodiazepine receptors in association with epileptic seizures in EL mice. Brain Res. 1996;717:91–8.
24. Shiotani T, Nakamoto Y, Watabe S, Yoshii M, Nabeshima T. Anticonvulsant actions of nefiracetam on epileptic EL mice and their relation to peripheral-type benzodiazepine receptors. Brain Res. 2000;859:255–61.
25. Soustiel JF, Glenn TC, Shik V, Boscardin J, Mahamid E, Zaaroor M. Monitoring of cerebral blood flow and metabolism in traumatic brain injury. J Neurotrauma. 2005;22:955–65.
26. Shohami E, Novikov M, Bass R. Long-term effect of HU-211, a novel non-competitive NMDA antagonist, on motor and memory functions after closed head injury in the rat. Brain Res. 1995;674:55–62.
27. Prins ML, Fujima LS, Hovda DA. Age-dependent reduction of cortical contusion volume by ketones after traumatic brain injury. J Neurosci Res. 2005;82:413–20.
28. Lifshitz J, Friberg H, Neumar RW, Raghupathi R, Welsh FA, Janmey P, *et al.* Structural and functional damage sustained by mitochondria after traumatic brain injury in the rat: evidence for differentially sensitive populations in the cortex and hippocampus. J Cereb Blood Flow Metab. 2003;23:219–31.
29. Johnston AJ, Steiner LA, Coles JP, Chatfield DA, Fryer TD, Smielewski P, *et al.* Effect of cerebral perfusion pressure augmentation on regional oxygenation and metabolism after head injury. Crit Care Med. 2005;33:189–95. discussion 255–187.
30. Belli A, Sen J, Petzold A, Russo S, Kitchen N, Smith M. Metabolic failure precedes intracranial pressure rises in traumatic brain injury: a microdialysis study. Acta Neurochir (Wien). 2008;150:461–9. discussion 470.
31. Enblad P, Valtysson J, Andersson J, Lilja A, Valind S, Antoni G, *et al.* Simultaneous intracerebral microdialysis and positron emission tomography in the detection of ischemia in patients with subarachnoid hemorrhage. J Cereb Blood Flow Metab. 1996;16:637–44.
32. Hillered L, Persson L, Nilsson P, Ronne-Engstrom E, Enblad P. Continuous monitoring of cerebral metabolism in traumatic brain injury: a focus on cerebral microdialysis. Curr Opin Crit Care. 2006;12:112–8.
33. Hlatky R, Valadka AB, Goodman JC, Robertson CS. Evolution of brain tissue injury after evacuation of acute traumatic subdural hematomas. Neurosurgery. 2004;55:1318–23. discussion 1324.
34. Langemann H, Mendelowitsch A, Landolt H, Alessandri B, Gratzl O. Experimental and clinical monitoring of glucose by microdialysis. Clin Neurol Neurosurg. 1995;97:149–55.
35. Valtysson J, Persson L, Hillered L. Extracellular ischaemia markers in repeated global ischaemia and secondary hypoxaemia

monitored by microdialysis in rat brain. Acta Neurochir (Wien). 1998;140:387–95.
36. Bazan Jr NG, Rakowski H. Increased levels of brain free fatty acids after electroconvulsive shock. Life Sci. 1970;9:501–7.
37. Gercken G, Brauning C. Quantitative determination of hydrolysis products of phospholipids in the ischaemic rat brain. Pflugers Arch. 1973;344:207–15.
38. Chan PH, Longar S, Fishman RA. Phospholipid degradation and edema development in cold-injured rat brain. Brain Res. 1983;277:329–37.
39. Veiga S, Azcoitia I, Garcia-Segura LM. Ro5-4864, a peripheral benzodiazepine receptor ligand, reduces reactive gliosis and protects hippocampal hilar neurons from kainic acid excitotoxicity. J Neurosci Res. 2005;80:129–37.